

# Spin-coupled molecular orbitals: chemical intuition meets quantum chemistry

Daniel Marti-Dafcik,<sup>1,\*</sup> Nicholas Lee,<sup>1</sup> Hugh G. A. Burton,<sup>1,2,</sup> David P. Tew<sup>1,†</sup>

<sup>1</sup>*Physical and Theoretical Chemistry Laboratory, University of Oxford, South Parks Road, Oxford, OX1 3QZ, UK*

<sup>2</sup>*Yusuf Hamied Department of Chemistry, University of Cambridge, Lensfield Road, Cambridge, CB2 1EW, UK*

(Dated: February 15, 2024)

Molecular orbital theory is powerful both as a conceptual tool for understanding chemical bonding, and as a theoretical framework for ab initio quantum chemistry. Despite its undoubted success, MO theory has well documented shortcomings, most notably that it fails to correctly describe di-radical states and homolytic bond fission. In this contribution, we introduce a generalised MO theory that includes spin-coupled radical states. We show through archetypical examples that when bonds break, the electronic state transitions between a small number of valence configurations, characterised by occupation of both delocalised molecular orbitals and spin-coupled localised orbitals. Our theory provides a model for chemical bonding that is both chemically intuitive and qualitatively accurate when combined with ab initio theory. Although exploitation of our theory presents significant challenges for classical computing, the predictable structure of spin-coupled states is ideally suited to algorithms that exploit quantum computers. Our approach provides a systematic route to overcoming the initial state overlap problem and unlocking the potential of quantum computational chemistry.

## I. INTRODUCTION

Solving Schrödinger’s equation to characterise the electronic structure of molecules and compute the Born–Oppenheimer potential energy surface remains a central goal of quantum chemistry. Modern electronic structure theory has arisen from nearly a century of sustained research and development, and the vast majority of modern methods are based on Molecular Orbital (MO) theory,[1–4] either in the form of Kohn–Sham Density Functional Theory[5] or post-Hartree–Fock correlation methods.[6] These approaches came to prominence in no small part due to the natural mapping of the MO representation of the many-electron wavefunction to linear algebra and matrix operations that can be performed with high efficiency on classical digital computers.[7, 8]

Despite the success of MO theory, it has well-documented shortcomings.[9–12] Closed-shell ground states are typically well approximated by a single configuration of electrons in spin-orbitals, but open-shell states, or cases with many competing low-energy configurations, are not. In practice, the accurate description of fundamental chemical processes, such as bond breaking using MO theory, requires a very large number of excited configurations,[13, 14] and sophisticated optimisation techniques.[15–18] As a consequence, any connection between simple chemical models and data from high-level ab initio calculations is obfuscated.

Looking to the future, it is increasingly probable that quantum computers will become available for scientific computing.[19–23] Many of the constraints on the way that many-electron wavefunctions are represented and optimised in modern MO-based theories do not apply to

quantum algorithms and we were therefore motivated to examine the electronic structure of bond formation and breaking afresh.

In this article, we introduce a generalised MO theory that includes spin-coupled radical states. Our theory provides a chemically intuitive picture of bonding that directly maps to a highly compact representation of the many-body wavefunction. Contrary to the current consensus among the electronic structure community, we find that it is not necessary to use sophisticated multi-reference expansions with very large numbers of variational parameters to describe bond breaking. Instead, we show that the electronic state undergoes transitions between a small number of valence states, each with an easily understood spin-coupled electronic configuration.

Furthermore, we show that our representation encodes strong correlation through prescribed patterns of entanglement, which is ideally suited to quantum computing. We demonstrate that our approach provides a powerful route to construct the sufficiently accurate reference states that are required for the practical application of fault-tolerant algorithms, such as quantum phase estimation[24–26] and related approaches.[27–31]

## II. MOLECULAR HYDROGEN

The prototypical chemical bond between two hydrogen atoms exemplifies the language and conceptual framework within which electronic structure theories operate. In MO theory, the left  $L$  and right  $R$   $1s$  atomic orbitals combine to form bonding  $\sigma_g$  and anti-bonding  $\sigma_u$  MOs that transform as the irreducible representations of the  $D_{\infty h}$  molecular point group.[3, 4] The wavefunction is written as the closed-shell singlet, doubly occupying the bonding MO, which is the Slater determinant used in Hartree–Fock theory  $|\Phi_{\text{RHF}}\rangle = |\sigma_g \bar{\sigma}_g\rangle$ . The MO description is accurate around the equilibrium bond length,

\* [dmartidafcik@gmail.com](mailto:dmartidafcik@gmail.com)

† [david.tew@chem.ox.ac.uk](mailto:david.tew@chem.ox.ac.uk)

but deteriorates as the molecule dissociates. This well-known failure arises from the inclusion of ionic terms in the wavefunction, which results from delocalised nature of the MOs[8]

$$|\Phi_{\text{RHF}}\rangle = \frac{1}{2} \left( \underbrace{|s_L \bar{s}_L\rangle + |s_R \bar{s}_R\rangle}_{\text{ionic}} + \underbrace{|s_L \bar{s}_R\rangle - |\bar{s}_L s_R\rangle}_{\text{covalent}} \right). \quad (1)$$

The strong correlation that localises the electrons on opposite atoms is absent in the MO picture. In MO-based theories, this strong correlation is introduced through mixing with excited configurations, and for  $\text{H}_2$  the correct behaviour for the binding curve is obtained using two configurations

$$|\Psi\rangle = c_1 |\sigma_g \bar{\sigma}_g\rangle + c_2 |\sigma_u \bar{\sigma}_u\rangle. \quad (2)$$

In the general case, the number of excited configurations required to recover the correct electronic structure grows exponentially with the number of localised electrons. Modern MO-based methods for strong correlation therefore typically employ sophisticated wavefunction representations to optimise large numbers of variational parameters.

An alternative representation that predates MO theory is the valence bond (VB) approach of Heitler and London.[32] The VB wavefunction is the open-shell singlet spin-coupled state of 1s electrons on each H atom

$$|\Phi_{\text{VB}}\rangle = \mathcal{N}(|s_L \bar{s}_R\rangle - |\bar{s}_L s_R\rangle). \quad (3)$$

where the normalisation constant  $\mathcal{N} = (2 + 2S_{LR}^2)^{-1/2}$  depends on the orbital overlap  $S_{LR} = \langle s_L | s_R \rangle$ . The VB description also captures the bonding interaction, which arises through electron delocalisation resulting from the overlap of the  $L$  and  $R$  1s orbitals. Approaches based on VB wavefunctions, however, are poorly suited to both classical and quantum computing due to reliance on non-orthogonal orbitals, which introduces cumbersome overlap terms in the working equations.[33–35]

Notwithstanding the differences in the MO and VB representations, the physical process of bond breaking is clear: the electronic state transitions from a singlet spin-coupled bonding  $\sigma_g^2$  configuration in the equilibrium region to a singlet spin-coupled diradical  $s_L^1 s_R^1$  configuration at dissociation. On a classical digital computer, the basis transformations required to combine configurations of different orbitals are costly and often impractical. On a digital quantum computer, basis transformations pose no difficulty. Orbital rotations are encoded through products of exponentials of single excitation and de-excitation operators,[36] and the corresponding quantum circuits have linear depth in orbital number and minimal qubit connectivity.[21]

We therefore choose to generalise MO theory by expressing the wavefunction as a superposition of configurations where electrons occupy both delocalised MOs and localised AOs. This representation directly encodes both the covalent interactions responsible for bonding and the

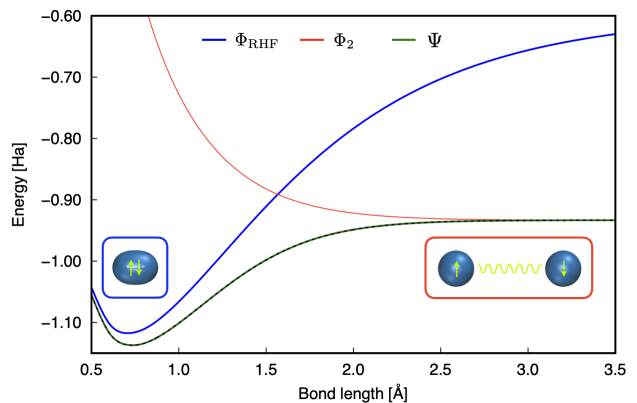


FIG. 1: Dissociation of  $\text{H}_2$  in the STO-3G basis using generalised spin-coupled orbitals.

the strong correlation that localises electrons at different sites, giving a physically accurate trial wavefunction across the whole binding curve without requiring large numbers of variational parameters.

For  $\text{H}_2$ , the singlet coupled  $s_L s_R$  diradical state is

$$|\Phi_2\rangle = \frac{1}{\sqrt{2}}(|s_L \bar{s}_R\rangle - |\bar{s}_L s_R\rangle) = \frac{1}{\sqrt{2}}(|\sigma_g \bar{\sigma}_g\rangle - |\sigma_u \bar{\sigma}_u\rangle). \quad (4)$$

where now  $s_L = \frac{1}{\sqrt{2}}(\sigma_g + \sigma_u)$  and  $s_R = \frac{1}{\sqrt{2}}(\sigma_g - \sigma_u)$  are orthogonal orbitals localised on the left and right atoms. In contrast to the Heitler–London wavefunction, this is a purely repulsive state.[37] The correct binding curve (Figure 1) is obtained through the linear combination of the  $\sigma_g^2$  and  $s_L s_R$  states

$$|\Psi\rangle = c_1 |\Phi_{\text{RHF}}\rangle + c_2 |\Phi_2\rangle. \quad (5)$$

The  $|\Phi_{\text{RHF}}\rangle$  state is uncorrelated, since a single Slater determinant is an antisymmetrised orbital product corresponding to an independent electron wavefunction.  $|\Phi_2\rangle$  is an entangled, or strongly correlated state, since it is a linear combination of determinants that cannot be converted to a single determinant through orbital rotation. Both states have low complexity since their structures are determined by symmetry considerations. The weights of the entanglement structure in  $|\Phi_2\rangle$  are specified through the rules of spin angular momentum coupling to obtain a singlet spin molecular ground state.

In this representation, the bonding interaction arises through increasing character of the delocalised  $\sigma_g^2$  configuration, which is driven by the favourable kinetic energy of the delocalised state and the attractive electron-nucleus Coulomb interaction. Conversely, the dominant electron correlation process for the  $\text{H}_2$  bond is the localisation of the electrons on opposite atoms, introducing partial diradical character, and this correlation increases in strength as the bond length increases. This transition from delocalised to localised electronic states is equivalent to the metal-insulator transition in the Fermi–Hubbard model, where the  $\text{H}_2$  bond length plays a similar

role to the ratio  $U/t$  between the on-site repulsion  $U$  and the hopping term  $t$ .

In the following, we demonstrate how these simple concepts can be generalised to more complex cases where multiple bonds are broken. We show that the strongly correlated state at dissociation is highly structured and that the structure is determined solely by symmetry and spin-angular momentum coupling considerations. Furthermore, we show that the transition from the simple covalent equilibrium bonding structure to the strongly correlated dissociated state is represented by a small number of intermediate configurations, each with their own spin-coupled structure. We first summarise the configuration state functions that we use to represent spin-coupled open-shell configurations.

### III. CONFIGURATION STATE FUNCTIONS

The exact molecular wavefunction is an eigenstate of both the total spin angular momentum operator  $\hat{S}^2$  and the spin projection operator  $\hat{S}_z$  with quantum numbers  $S, M$ . A single Slater determinant, the many-electron basis function in MO-based theories, is an eigenfunction of  $\hat{S}_z$ , but not of  $\hat{S}^2$ , except for closed-shell and high-spin open-shell configurations. The physically relevant functions for describing open-shell states with localised orbitals are configuration state functions (CSF), which are eigenstates of  $\hat{S}^2$  with quantum numbers  $S, M$ .

A CSF is defined by a specification of the open-shell orbitals and a specification of the spin-coupling pattern, which is determined by the order and manner in which the spin- $\frac{1}{2}$  particles in the open-shell orbitals are coupled. Formally, our CSFs take the form

$$|\Phi\rangle = \mathcal{N}\hat{A}\left(|\phi_c\bar{\phi}_c\dots\rangle\mathcal{O}_{SM}^{N,i}(\phi_o\bar{\phi}_o\dots)\right). \quad (6)$$

where  $\hat{A}$  is the antisymmetric permutation operator,  $c$  denotes the doubly occupied closed-shell orbitals,  $o$  are the open-shell orbitals, and  $\mathcal{O}_{SM}^{N,i}(\phi_o\bar{\phi}_o\dots)$  is an open-shell state with  $N$  electrons in orbitals  $\{\phi_o, \bar{\phi}_o\}$  coupled with spin quantum numbers  $S$  and  $M$  in a spin-coupling pattern labelled by  $i$ , and  $\mathcal{N}$  is a normalisation constant. All occupied spin-orbitals are mutually orthogonal and normalised.

The open-shell state  $\mathcal{O}_{SM}^{N,i}$  for coupled angular momenta can be expressed in terms of the uncoupled Slater determinant representation of  $N$  electrons in open-shell orbitals  $\{\phi_o, \bar{\phi}_o\}$  through the Clebsch–Gordan coefficients for the spin-coupling pattern. A list of relevant CSF wavefunctions is provided in Appendix A.

To streamline presentation, we use a simplified notation for  $|\Phi\rangle$  in Eq 6, listing only the occupancy of the spatial orbitals and suppressing  $\hat{A}$  and  $\mathcal{N}$ :

$$|\Phi\rangle = |\phi_c^2\dots\rangle\mathcal{O}_{SM}^{N,i}(\phi_o\dots). \quad (7)$$

Classical digital approaches that use a CSF basis rather than a Slater determinant basis, such as spin-

adapted FCI quantum Monte Carlo,[38] are constrained to use one set of orbitals and one coupling scheme with an orthonormal basis of CSFs. This restriction allows Hamiltonian matrix elements to be evaluated using efficient group theoretical approaches without explicitly building the Slater determinant expansion of each CSF, which has exponential cost.[39, 40] Quantum algorithms are not constrained in this way and we are free to use orbitals and coupling patterns that directly encode the physical interactions. Furthermore, we can combine AO configurations for coupled high-spin atomic fragments with MO configurations for delocalised covalent bonds, as well as configurations intermediate between the these extremes.

The physical interactions follow established rules connected to the relative strengths of exchange and delocalisation energies, and the CSFs required to represent the electronic state compactly are straightforwardly constructed. For example, the electron configurations of dissociated atomic fragments follow Hund’s rules, where electron spins couple to form a local high-spin state, and the net electron spin angular momenta of the atoms couple to form low-spin states. Bonding interactions in the molecule are formed when paired electrons occupy delocalised molecular orbitals. We now illustrate this framework using examples that pose significant challenges for traditional approaches.

### IV. HOMOLYTIC BOND CLEAVAGE

#### A. Breaking a triple bond: N<sub>2</sub>

Dissociation of the nitrogen molecule is a well-documented challenge for electronic structure theory[41–51] because the six electrons in the triple bond become very strongly correlated when the bond elongates. Even when only considering the six 2p valence orbitals[52] there are 56 Slater determinants with the correct symmetry that contribute to the wavefunction. However, using generalised MO theory, the wavefunction is recovered to better than 92% across the whole binding curve with only four CSFs (Figure 2).

MO theory predicts a  $1\sigma_g^21\sigma_u^22\sigma_g^22\sigma_u^23\sigma_g^21\pi_u^4$  configuration for the N<sub>2</sub> molecule, with a  $^1\Sigma_g^+$  ground state. The corresponding CSF is simply the closed-shell Hartree–Fock wavefunction

$$|\Phi_{\text{RHF}}\rangle = |\mathcal{C}\rangle|3\sigma_g^21\pi_{u,x}^21\pi_{u,y}^2\rangle \quad (8)$$

where  $|\mathcal{C}\rangle = |1\sigma_g^21\sigma_u^22\sigma_g^22\sigma_u^2\rangle$  is the contribution from the core orbitals that are not involved in bonding. At dissociation, each atom has a  $1s^22s^22p^3$  electronic configuration with spins locally coupled to a  $^4P$  on each atom, which then couple through space to give a  $^1\Sigma_g^+$  molecular state with the CSF structure

$$|\Phi_6\rangle = |\mathcal{C}\rangle\mathcal{O}_{00}^{6,1}(xLY_LzLxRY_RzR) \quad (9)$$

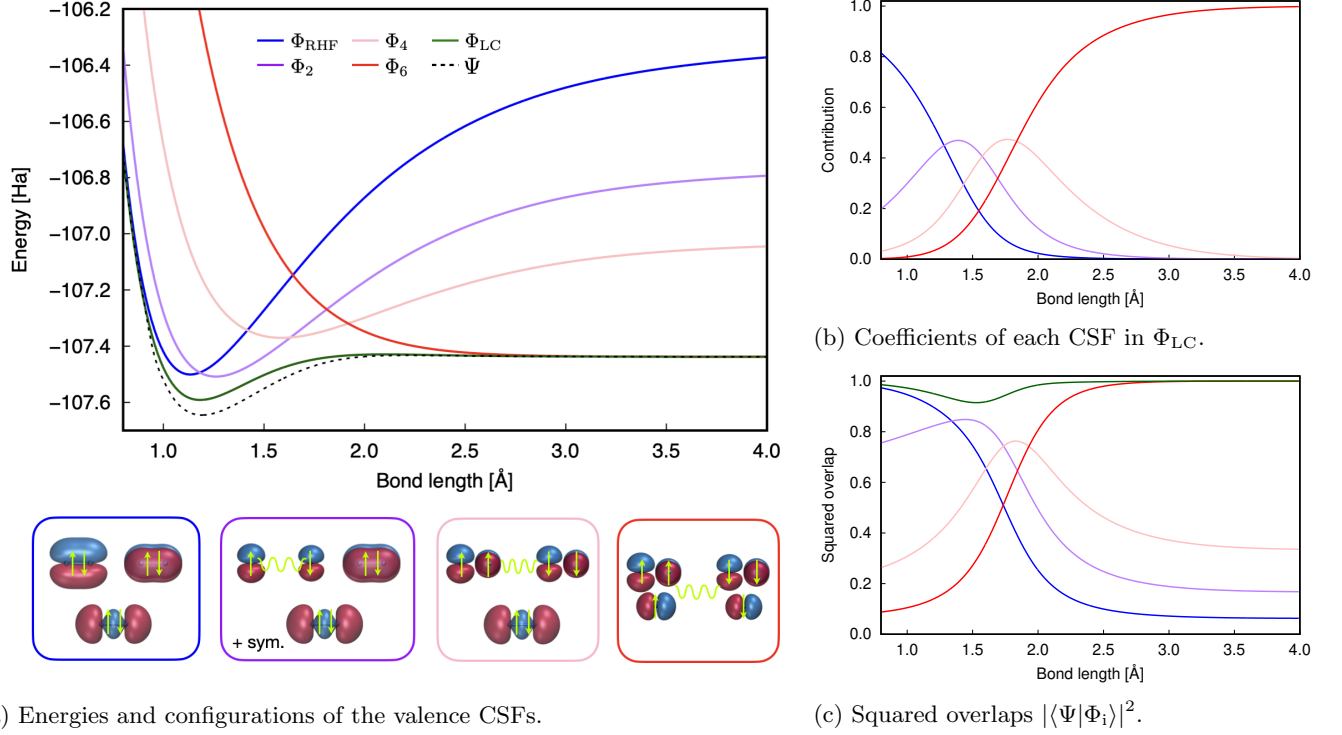


FIG. 2: The dissociation of  $N_2$  in a STO-3G basis in the six  $2p$  valence space using generalised MO theory.

where  $z_L = \frac{1}{\sqrt{2}}(3\sigma_g + 3\sigma_u)$ ,  $z_R = \frac{1}{\sqrt{2}}(3\sigma_g - 3\sigma_u)$ ,  $x_L = \frac{1}{\sqrt{2}}(1\pi_{u,x} + 1\pi_{g,x})$ ,  $x_R = \frac{1}{\sqrt{2}}(1\pi_{u,x} - 1\pi_{g,x})$  etc are localised atomic orbitals. The spin function  $\mathcal{O}_{00}^{6,1}$  spin-couples the three-electron quartets on each atom into a singlet, and is a specific linear combination of 20 open-shell determinants [Eq. (A6)]. The closed-shell part  $|\mathcal{C}\rangle$  is invariant to rotations among its constituent orbitals making it equal to  $|1s_L^2 1s_R^2 2s_L^2 2s_R^2\rangle$ . As the bond elongates, one  $\pi$  bond breaks first, then both  $\pi$  bonds, and finally the  $\sigma$  bond. The CSFs that describe these intermediate states with one and two broken bonds are

$$|\Phi_4\rangle = |\mathcal{C}\rangle |\sigma_g^2\rangle \mathcal{O}_{00}^{4,1}(x_L y_L x_R y_R) \quad (10)$$

$$|\Phi_2\rangle = |\Phi_{2x}\rangle + |\Phi_{2y}\rangle \quad (11)$$

$$|\Phi_{2x}\rangle = |\mathcal{C}\rangle |\sigma_g^2 \pi_{u,y}^2\rangle \mathcal{O}_{00}^{2,1}(x_L x_R) \quad (12)$$

$$|\Phi_{2y}\rangle = |\mathcal{C}\rangle |\sigma_g^2 \pi_{u,x}^2\rangle \mathcal{O}_{00}^{2,1}(y_L y_R) \quad (13)$$

where  $|\Phi_{2x}\rangle$  and  $|\Phi_{2y}\rangle$  are a degenerate pair. The state  $\mathcal{O}_{00}^{4,1}$  describes atomic triplet states coupled to form a singlet overall and  $\mathcal{O}_{00}^{2,1}$  describes atomic doublet states coupled to a singlet. The representations of  $\mathcal{O}_{00}^{6,1}$ ,  $\mathcal{O}_{00}^{4,1}$  and  $\mathcal{O}_{00}^{2,1}$  in terms of Slater determinants are collected in Appendix A. In this formulation, the localised orbitals  $x_L, x_R, y_L, y_R, z_L, z_R$  are mutually orthogonal and are therefore not true atomic orbitals except at infinite separation.

Just as for  $H_2$ , the RHF state dissociates to the incorrect limit due to the presence of unphysical ionic terms in

the wavefunction, and the exact dissociated state is the CSF where the high-spin atomic states couple to form a singlet (Figure 2a). The CSFs with bond orders of two and one behave similarly to the RHF state but with higher energy in the bonding region, lower ionic destabilisation at dissociation, and with minima at progressively longer bond lengths, entirely consistent with their bonding character. The closed-shell orbitals used in these CSFs were obtained from the RHF wavefunction, but very similar curves are obtained if the orbitals of each CSF are relaxed, for example through RASSCF optimisation (restricted active space self consistent field).[53]

Figure 2a also displays the energy of the exact ground state in the (6e,6o) active space of the bonding electrons and the energy obtained from the variationally optimised linear combination of the four valence CSFs. The optimised coefficients and the overlap of each state with the exact ground state are displayed in figures 2b and 2c.

While the optimised linear combination of these four CSFs is dominated by the RHF configuration at equilibrium, electrons in a bond correlate by localising on opposite atoms, occupying low-energy spin-coupled states, leading to non-negligible contributions from the CSFs with lower bond orders and an equilibrium bond length longer than that of the RHF state. Just as for  $H_2$ , the strength of these correlation processes increases as the bond elongates. In this formulation, only four CSFs are required to obtain an accurate binding curve with an overlap with the exact state of at least 92% at all bond lengths. The largest deviations are found in the bond-

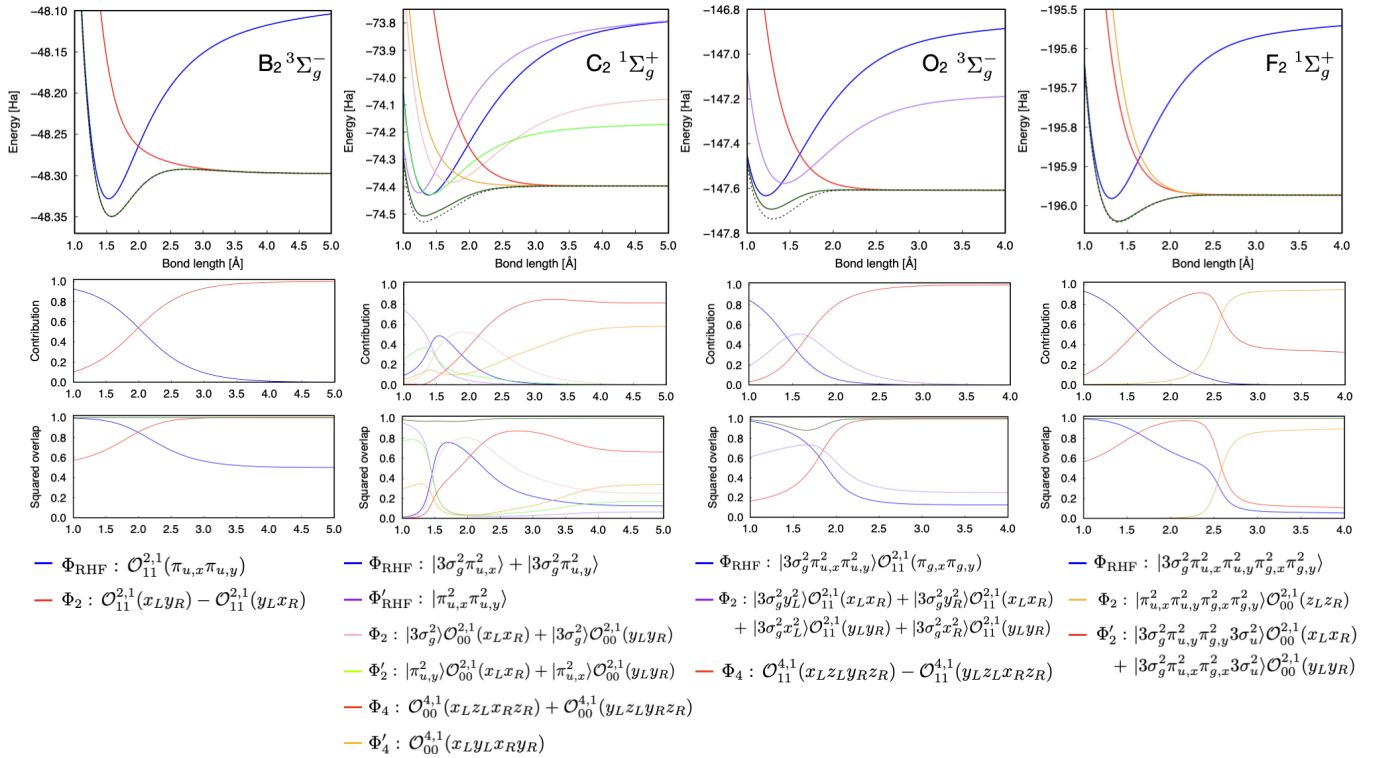


FIG. 3: CSF energies, configurations and weights in the binding of first row diatomics.

ing region where there is significant additional dynamic correlation among the six electrons in the triple bond.

The state at dissociation is strongly correlated in the sense that the electrons are localised on opposite atoms, and is a linear combination of 20 Slater determinants. However, this state is described exactly by a single CSF. The complexity is low; the coefficients in the determinantal representation are determined entirely by symmetry and spin angular momentum considerations.

Our generalised spin-coupled MO theory provides a highly intuitive description of chemical bonding that maps directly onto clearly identifiable contributions to the many-electron wavefunction. Since each contribution is composed of different orbitals (localised and covalent) and different spin-coupling patterns, the states are non-orthogonal and optimisation of the linear combination requires non-orthogonal configuration interaction (CI) theory.[54–58] In the context of fault-tolerant quantum algorithms, such as quantum phase estimation, using  $|\Phi_{\text{LC}}\rangle$  as the reference wavefunction instead of  $|\Phi_{\text{RHF}}\rangle$  translates into more than an order of magnitude reduction in runtime at stretched geometries (see Section VI).

## B. First row diatomics

Our spin-coupled generalised MO formalism is straightforwardly generalised to the bonding motifs of all of the first-row diatomic molecules, irrespective of whether the electronic ground state is singlet or triplet

spin-coupled. Starting from the HF state given by standard MO theory, CSFs with incrementally lower bond order are generated by localising the electrons in the weakest remaining bond into the corresponding non-bonding atomic orbitals. The spin coupling pattern follows Hund’s rules, where electrons first spin-couple with other unpaired electrons on the same atom to give high-spin atomic states, which then spin-couple to give the appropriate overall spin state for the molecule. The  $D_{\infty h}$  molecular point group symmetry is satisfied by taking the symmetry adapted linear combinations generated by the symmetry operations.

In Figure 3 we plot the potential energy curves for the valence CSFs and the accuracy of the linear combination with respect to full CI in the  $(Ne, 6o)$  active space for  $B_2$ ,  $C_2$ ,  $O_2$  and  $F_2$ . The CSFs are also listed. In all cases accurate binding curves and overlap with the FCI state of at least 88% are obtained, with the largest deviation for the bonding region of  $O_2$  where significant additional dynamic correlation contributes. The triplet state  $B_2$  transitions from the  $\pi^2$  single-bond configuration to a triplet diradical state at dissociation. For  $C_2$ , configurations with either  $\sigma$  or  $\pi$  occupation are both important since the large sp mixing, arising from the small s-p orbital energy gap, destabilises the  $\sigma$  configurations. In the dissociation limit, the ground state tends towards the spin-coupled atomic states, where the electrons are evenly distributed among the  $p_x, p_y, p_z$  orbitals. This is also the reason that  $F_2$  requires both the  $\sigma$ -hole and  $\pi$ -hole configurations at dissociation. The triplet state  $O_2$

follows exactly the same physical rules, but the three spin-coupled states contain multiple symmetry-related components.

### C. Breaking two single bonds: H<sub>2</sub>O

The symmetric dissociation of H<sub>2</sub>O is another challenging case for electronic structure theory, involving strong correlation and spin-coupling among the electrons as the bonds break.[59, 60] In contrast to N<sub>2</sub>, the dissociation of H<sub>2</sub>O involves the localisation of electrons onto more than two sites.

The MO description of water leads to the configuration  $1a_1^2 2a_1^2 1b_2^2 3a_1^2 1b_1^2$ , with term symbol  $^1A_1$ , where the  $x$ -axis points out of the plane of the molecule. The closed-shell orbitals form the state  $|\mathcal{C}\rangle = |1a_1^2 2a_1^2 1b_1^2\rangle$ , which contains the 1s, 2s and  $2p_x$  orbitals on the oxygen atom, and the RHF wavefunction is

$$|\Phi_{\text{RHF}}\rangle = |\mathcal{C}\rangle |1b_2^2 3a_1^2\rangle = |\mathcal{C}\rangle |\sigma_L^2 \sigma_R^2\rangle \quad (14)$$

where  $\sigma_L$  and  $\sigma_R$  are MOs localised on the left and right OH bonds. The CSF for the dissociated state is that where the oxygen electrons from the two cleaved OH

bonds spin-couple to form a triplet oxygen state, due to the favourable exchange stabilisation, meaning that the two hydrogen electrons must also spin-couple to form a triplet and these triplets spin-couple to form the singlet molecular state:

$$|\Phi_4\rangle = |\mathcal{C}\rangle \mathcal{O}_{00}^{4,1}(o_L o_R h_L h_R) \quad (15)$$

where, in a minimal basis, the localised orbitals are obtained through simple rotation of the valence orbitals

$$\begin{aligned} o_L &= (\sigma_L + \sigma_L^*)/\sqrt{2}, & o_R &= (\sigma_R + \sigma_R^*)/\sqrt{2} \\ h_L &= (\sigma_L - \sigma_L^*)/\sqrt{2}, & h_R &= (\sigma_R - \sigma_R^*)/\sqrt{2} \\ \sigma_L &= (1b_2 + 3a_1)/\sqrt{2}, & \sigma_L^* &= (2b_2 + 4a_1)/\sqrt{2} \\ \sigma_R &= (1b_2 - 3a_1)/\sqrt{2}, & \sigma_R^* &= (2b_2 - 4a_1)/\sqrt{2} \end{aligned} \quad (16)$$

The CSF that describes the intermediate configuration between the fully bonded and fully dissociated states includes one broken OH bond. The molecular point group symmetry demands that this state must be a symmetric superposition of the left and right bonded configurations, which results in

$$|\Phi_2\rangle = |\mathcal{C}\rangle |\sigma_L^2\rangle \mathcal{O}_{00}^{2,1}(o_R h_R) + |\mathcal{C}\rangle |\sigma_R^2\rangle \mathcal{O}_{00}^{2,1}(o_L h_L) \quad (17)$$

The relative contributions of each CSF to a variationally optimised linear combination follow the intuitive trend, transitioning from the RHF state at equilibrium to  $|\Phi_4\rangle$  at dissociation (Figure 4). Remarkably, the electron correlation is almost entirely captured by the three CSFs at all bond lengths, and the squared overlap with the exact wavefunction is at least 99% everywhere. At intermediate bond lengths all three CSFs have approximately equal contributions, which coincides with the region where traditional algorithms encounter the most difficulties.

### V. HYDROGEN CHAINS: H<sub>4</sub>

The change in the electronic structure of hydrogen chains as the separation increases is another challenging case for electronic structure theory. This simple system can be used to understand conjugation in  $\pi$  systems and is closely related to the Hubbard model for metal-to-insulator transitions in materials.[61]

We start with the cyclic H<sub>4</sub> structure, which shares electronic structure characteristics with the  $\pi$  system of cyclobutadiene in a square geometry, and has a degenerate LUMO. In a minimal basis, the MOs are uniquely determined by symmetry and are the set  $a_{1g}, e_{u,x}, e_{u,y}, b_{2g}$ . We consider the open-shell singlet  $^1A_{1g}$ , which cannot be represented by a Slater determinant and is the CSF

$$|\Phi_0\rangle = |a_{1g}^2 e_{u,x}\rangle + |a_{1g}^2 e_{u,y}\rangle \quad (18)$$

where the  $x$  and  $y$  axes pass through the sides of the square. Following our reasoning that the next most

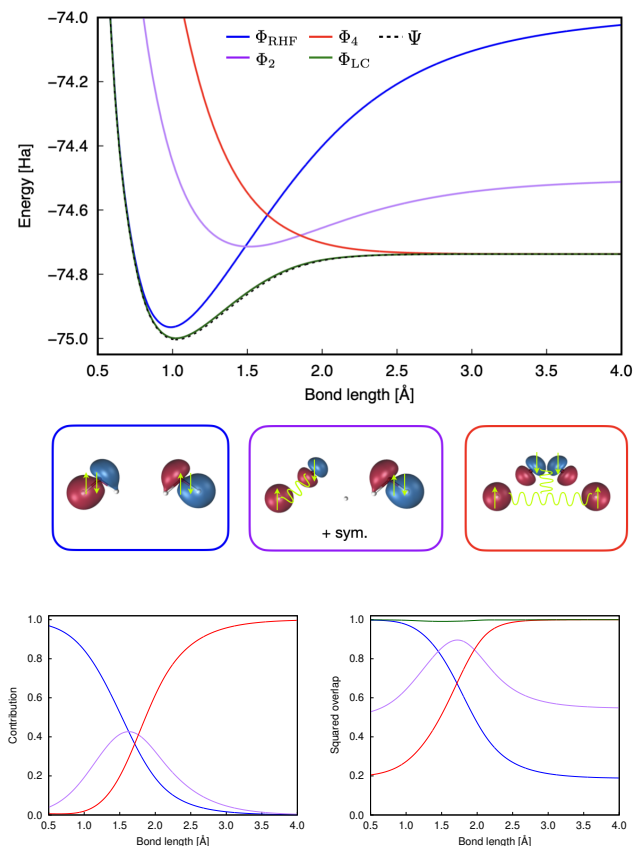


FIG. 4: Dissociation of H<sub>2</sub>O in a STO-3G basis using generalised spin-coupled orbitals.

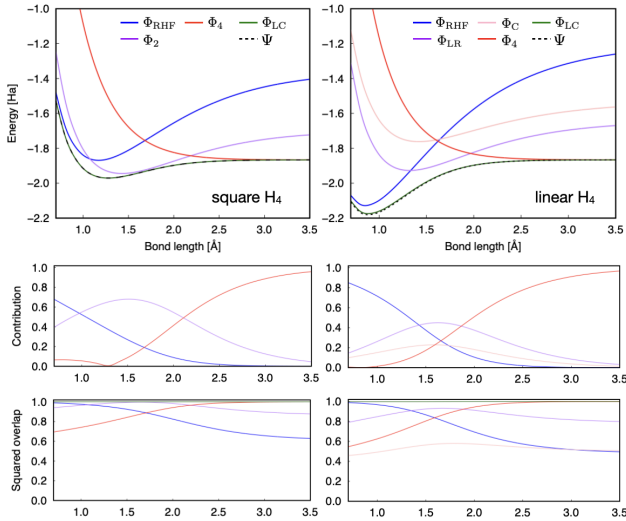


FIG. 5: Dissociation of square and linear  $H_4$  in a STO-3G basis.

important configurations are those where spins localise, we introduce bonding and antibonding orbitals localised on each of the four edges, left, right, top and bottom, through transformation of the valence orbitals

$$\begin{aligned}
 \sigma_L &= (a_{1g} + e_{u,x})/\sqrt{2}, & \sigma_L^* &= (b_{2g} + e_{u,x})/\sqrt{2} \\
 \sigma_R &= (a_{1g} - e_{u,x})/\sqrt{2}, & \sigma_R^* &= (b_{2g} - e_{u,x})/\sqrt{2} \\
 \sigma_T &= (a_{1g} + e_{u,y})/\sqrt{2}, & \sigma_T^* &= (b_{2g} + e_{u,y})/\sqrt{2} \\
 \sigma_B &= (a_{1g} - e_{u,y})/\sqrt{2}, & \sigma_B^* &= (b_{2g} - e_{u,y})/\sqrt{2}
 \end{aligned} \tag{19}$$

The atomic 1s orbitals are recovered by taking linear combinations of bonding and antibonding pairs. The CSF that describes the valence state with partial localised bonding is

$$\begin{aligned}
 |\Phi_2\rangle &= |\sigma_L^2\rangle \mathcal{O}_{00}^{2,1}(s_3, s_4) + |\sigma_R^2\rangle \mathcal{O}_{00}^{2,1}(s_1, s_2) \\
 &\quad + |\sigma_T^2\rangle \mathcal{O}_{00}^{2,1}(s_1, s_4) + |\sigma_B^2\rangle \mathcal{O}_{00}^{2,1}(s_2, s_3)
 \end{aligned} \tag{20}$$

and the CSF for the fully open-shell state is

$$|\Phi_4\rangle = \mathcal{O}_{00}^{4,2}(s_1, s_2, s_3, s_4) + \mathcal{O}_{00}^{4,2}(s_2, s_3, s_4, s_1) \tag{21}$$

where  $\mathcal{O}_{00}^{4,2}$  is the antisymmetrised product of two open-shell singlets (Eq A4). In Figure 5 we present the binding curves for the symmetric dissociation of  $H_4$ . These three valence states are sufficient to reproduce the exact binding curve and represent all of the correlation processes involved.

We now turn to the linear  $H_4$ , which shares electronic characteristics with the  $\pi$  system of butadiene. The valence states for linear  $H_4$  are the same as those of the cyclic structure, but where left-right and top-bottom symmetry was present in the square geometry it is now lost, becoming the left-right and centre-edge. The left-right and centre contributions to  $|\Phi_2\rangle$  must be included

separately, and the edge contributions become unimportant since they are non-bonding. At the dissociation limit, all  $2^4$  spin states with one electron on each atom are degenerate, but the degeneracy is lifted by the kinetic energy of delocalisation at finite separations. The state  $|\Phi_4\rangle$  is the linear combination of  $S = 0$  CSFs with maximal nearest neighbour delocalisation energy, and equivalently, minimal nearest neighbour spin coupling  $\langle \Phi | \hat{S}_i \cdot \hat{S}_j | \Phi \rangle$  through the isomorphism with the Heisenberg–Dirac spin Hamiltonian.[62–64]

## VI. QUANTUM COMPUTATION USING SPIN-COUPLED STATES

In digital quantum computing, the many-electron wavefunction is encoded by mapping it to a quantum superposition of the qubit states of the quantum device. Quantum algorithms involve preparing the initial qubit state for a known reference wavefunction  $|\Phi_{\text{ref}}\rangle$ , and either operating on it to drive it to ground state of the Hamiltonian  $|\Psi\rangle$ , for example in quantum imaginary time-evolution[65] and adiabatic state preparation,[24] or time-evolving it to extract the ground state energy through probabilistic projective measurements, for example in quantum phase estimation (QPE).[24–26, 66] The cost of these approaches depends critically on the overlap of the initial reference state with the exact ground state wavefunction.[67]

In QPE, for example, the probability of measuring the ground state energy is determined by the squared overlap  $\gamma^2 = |\langle \Phi_{\text{ref}} | \Psi \rangle|^2$ . Consequently,  $\mathcal{O}(|\gamma|^{-2})$  measurements are required to obtain the ground state energy reliably. This overlap problem remains significant despite the tremendous progress over the past two decades, which has reduced the quantum circuit cost (number of operations) required to implement time-evolution to scale approximately quadratically with the number of orbitals,[68–71] and has seen the emergence of post-QPE approaches requiring  $\mathcal{O}(|\gamma|^{-1})$  measurements.[27–29].

Most implementations of quantum algorithms employ the Hartree–Fock state as the reference.[72] However, since the overlap between the Hartree–Fock determinant and the exact ground state decays exponentially with the number of open-shell electrons, the performance of subsequent quantum algorithms for strongly-correlated systems rapidly deteriorates.[67] Several works on concrete resource estimates for QPE-based electronic structure for challenging systems predict runtimes for a single-point energy calculation in the order of several days, despite generous assumptions for the quantum hardware requirements.[19, 70, 73] It is clear that reductions in the overall runtime of QPE, as enabled through improved reference states, are of paramount importance to enable practical quantum computation of electronic structure.

Our spin-coupled formalism provides a systematic approach to constructing reference wavefunctions with good overlaps with the exact state, and therefore has the po-

tential to unlock the power of quantum algorithms for challenging chemical problems.[19, 71, 74] Our approach is ideally suited to quantum computing. Although the number of determinants in each CSF is equal to the number of fully open-shell determinants with  $M_s = 0$ , which grows combinatorially with the size of the system as  $\binom{N}{N/2}$ , [39] the number of distinct coefficients only scales as  $\mathcal{O}(N)$ . Their prescribed entanglement structure means that they can be efficiently prepared on a quantum device, with a cost negligible to that of quantum algorithms.[75] Similarly, the fact that each contributing valence state uses different sets of orthonormal orbitals, and that the valence states are not mutually orthogonal, poses no problem for quantum state preparation.[75] Using our reference wavefunctions as initial states in QPE directly reduces the overall runtime. In the simple case of  $N_2$ , for example,  $|\langle \Phi_{\text{RHF}} | \Psi \rangle|^2 \sim 0.06$  at elongated bonds, but  $|\langle \Phi_{\text{LC}} | \Psi \rangle|^2 \sim 1$  (Fig. 2c), which translates to a sixteen-fold speed-up in QPE execution.

Quantitative quantum chemical predictions[76] require the simultaneous treatment of strongly interacting states, dynamic correlation and orbital relaxation. Where classical methods fail due to problems of complexity,[77] the quantum approach extends straightforwardly. The orbitals for each configuration can be optimised in a large basis on a classical computer using RASSCF techniques at only mean-field cost. The linear coefficients of the accurate reference state can be computed in the same manner as quantum subspace algorithms,[78, 79] where each pair of CSFs is prepared on the quantum computer and overlap and Hamiltonian matrix elements obtained through measurement. Since the reference state directly encodes a large part of the entanglement structure of electronic ground states, a high-quality ground state energy can be extracted efficiently through QPE.

## VII. CONCLUSIONS AND OUTLOOK

Despite the fact that the chemical bond is at the very heart of chemical theory, an accurate representation of the process of bond formation has presented a severe challenge to quantum chemical methods. Modern approaches[77, 80–83] are based on complete expansions within a set of active MOs[13] and suffer from high computational and operational complexity, which has encouraged the widespread erroneous belief that the wavefunction is inherently complex. Using the spin-coupled molecular orbital theory presented in this article, we have shown that the wavefunction is in fact highly structured and that bond formation can be represented through a handful of spin-coupled states, each with well-defined spin quantum numbers and physical characteristics.

Our spin-coupled theory exposes a simple interpretation of the chemical bond. The character of the bond at equilibrium bond lengths is predominantly that predicted by MO theory, but electron crowding is relieved by diradical character, where electrons localise on opposite

atoms, leading to a reduction in formal bond order and bond elongation. As a bond breaks, the diradical character increases and the MO character reduces. For multiple bonds, the radical states are characterised by high-spin coupling of the electrons localised on each atom. The  $\sigma$  and  $\pi$  bonds break at different bond lengths, with the  $\pi$  bonds typically breaking first, and the bond order reduces sequentially as each pair of electrons in the bonds localise on opposite atoms. Applying this simple theory recovers 90% of the wavefunction resulting from a complete active space calculation, and our simple chemical model therefore has a direct connection to sophisticated wavefunction expansions.

Our model invokes different orbitals for each configuration, and the resulting states are not orthogonal. Moreover, the spin-coupled configurations correspond to different genealogical spin-coupling schemes, with different orbital orderings. The highly compact representation of the wavefunction afforded by our approach is lost when either a single orbital basis, or single CSF basis is used to represent all contributing states. For the archetypical strongly correlated systems considered in this work, the apparent complexity of the wavefunction in traditional approaches arises from the insistence on using a single basis of orthonormal orbitals and a single CSF basis to represent all configurations, so that the Hamiltonian matrix evaluation is straightforward.[6, 39, 40] While matrix elements between nonorthogonal Slater determinants can be readily computed,[84–86] building the determinant expansion of each CSF has exponential cost using traditional algorithms. To exploit the compact structure revealed by our theory, it is necessary to use methods that can handle non-orthogonal CSF states.

Quantum computing has the potential to overcome many of the remaining challenges in quantum chemistry. Provided that a high-quality reference state can be efficiently parametrised as a quantum circuit, algorithms such as quantum phase estimation and quantum eigenstate filtering can efficiently extract the exact ground state within a given basis set. Our spin-coupled molecular orbital theory provides a framework for constructing highly entangled reference states for strongly correlated molecular ground states using only a basic understanding of a chemical process, a small number of variational parameters, and at the cost of a mean-field calculation. Since the entanglement structure of each configuration is defined through spin and symmetry constraints, they can be prepared and transformed on a quantum register with low-depth quantum circuits, providing a practical route to using quantum algorithms to address challenging problems in quantum chemistry.

## ACKNOWLEDGMENTS

D.M.D. thanks Alexander Gunasekera for providing helpful suggestions and discussing several aspects of this work, and acknowledges financial support by the



EPSRC Hub in Quantum Computing and Simulation (EP/T001062/1). H.G.A.B. acknowledges financial support from New College, Oxford (Astor Junior Research Fellowship) and Downing College, Cambridge (Kim and Julianna Silverman Research Fellowship).

### Appendix A: Spin eigenfunctions

A CSF  $\mathcal{O}_{SM}^{N,i}(\phi_1 \dots \phi_N)$  has  $N$  electrons in spatial orbitals  $\{\phi\}$  and is a spin eigenfunction with quantum numbers  $S$  and  $M$ . Each CSF is a linear combination of determinants, here represented through the  $\alpha$  or  $\beta$  occupation of the orbitals  $\phi$ .

$$|\mathcal{O}_{0,0}^{2,1}\rangle = \frac{1}{\sqrt{2}}(|\alpha\beta\rangle - |\beta\alpha\rangle), \quad (\text{A1})$$

$$|\mathcal{O}_{1,1}^{2,1}\rangle = |\alpha\alpha\rangle, \quad (\text{A2})$$

$$|\mathcal{O}_{0,0}^{4,1}\rangle = \frac{1}{\sqrt{3}}(|\alpha\alpha\beta\beta\rangle + |\beta\beta\alpha\alpha\rangle) - \frac{1}{2\sqrt{3}}(|\alpha\beta\alpha\beta\rangle + |\beta\alpha\beta\alpha\rangle + |\alpha\beta\beta\alpha\rangle + |\beta\alpha\alpha\beta\rangle), \quad (\text{A3})$$

$$|\mathcal{O}_{0,0}^{4,2}\rangle = \frac{1}{2}(|\alpha\beta\alpha\beta\rangle - |\alpha\beta\beta\alpha\rangle - |\beta\alpha\alpha\beta\rangle + |\beta\alpha\beta\alpha\rangle), \quad (\text{A4})$$

$$|\mathcal{O}_{1,1}^{4,1}\rangle = \frac{1}{2}(|\alpha\alpha\alpha\beta\rangle - |\alpha\alpha\beta\alpha\rangle - |\alpha\beta\alpha\alpha\rangle + |\beta\alpha\alpha\alpha\rangle) \quad (\text{A5})$$

$$|\mathcal{O}_{0,0}^{6,1}\rangle = \frac{1}{2}(|\alpha\alpha\alpha\beta\beta\beta\rangle - |\beta\beta\beta\alpha\alpha\alpha\rangle) + \frac{1}{6}(|\alpha\beta\beta\alpha\alpha\beta\rangle + |\alpha\beta\beta\alpha\beta\alpha\rangle + |\alpha\beta\beta\beta\alpha\alpha\rangle + |\beta\beta\alpha\beta\alpha\alpha\rangle + |\beta\beta\alpha\alpha\beta\alpha\rangle + |\beta\beta\alpha\alpha\alpha\beta\rangle + |\beta\alpha\beta\beta\alpha\alpha\rangle + |\beta\alpha\beta\alpha\beta\alpha\rangle + |\beta\alpha\beta\alpha\alpha\beta\rangle - |\beta\alpha\alpha\beta\beta\alpha\rangle - |\beta\alpha\alpha\beta\alpha\beta\rangle - |\beta\alpha\alpha\alpha\beta\beta\rangle - |\alpha\beta\alpha\beta\beta\alpha\rangle - |\alpha\beta\alpha\beta\alpha\beta\rangle - |\alpha\beta\alpha\alpha\beta\beta\rangle - |\alpha\alpha\beta\beta\beta\alpha\rangle - |\alpha\alpha\beta\beta\alpha\beta\rangle), \quad (\text{A6})$$

### Appendix B: Computational details

We used PySCF to obtain the integrals and compute the RHF and FCI solution,[87, 88] and an in-house Python code for all other tasks, including: generating the spin eigenfunctions from the Clebsch-Gordan coupling coefficients, performing basis transformations, computing matrix elements and wavefunction overlaps, and solving the generalized eigenvalue problem. The visualization of the molecular orbitals was done using VMD.[89]

- 
- [1] R. S. Mulliken, The Assignment of Quantum Numbers for Electrons in Molecules. I, *Phys. Rev.* **32**, 186 (1928).
- [2] R. S. Mulliken, The Assignment of Quantum Numbers for Electrons in Molecules. II, *Phys. Rev.* **32**, 761 (1928).
- [3] J. E. Lennard-Jones, The determination of molecular orbitals, *Proceedings of the Royal Society of London. Series A. Mathematical and Physical Sciences* **198**, 1 (1949).
- [4] G. G. Hall, J. Lennard-Jones, The molecular orbital theory of chemical valency. iii. properties of molecular orbitals, *Proceedings of the Royal Society of London. Series A. Mathematical and Physical Sciences* **202**, 155 (1950).
- [5] W. Kohn, L. J. Sham, Self-consistent equations including exchange and correlation effects, *Physical Review* **140**, A1133 (1965).
- [6] T. Helgaker, P. Jørgensen, J. Olsen, *Molecular Electronic-Structure Theory* (John Wiley & Sons, 2000).
- [7] C. C. J. Roothaan, New Developments in Molecular Orbital Theory, *Rev. Mod. Phys.* **23**, 69 (1951).
- [8] J. C. Slater, Ferromagnetism and the band theory, *Rev. Mod. Phys.* **25**, 199 (1953).
- [9] P. Lykos, G. W. Pratt, Discussion on the hartree-fock approximation, *Reviews of Modern Physics* **35**, 496 (1963).
- [10] D. P. Tew, W. Klopper, T. Helgaker, Electron correlation: The many-body problem at the heart of chemistry, *Journal of Computational Chemistry* **28**, 1307 (2007).
- [11] J. C. Slater, Note on Molecular Structure, *Phys. Rev.* **41**, 255 (1932).
- [12] P. C. Varras, P. S. Gritzapis, The Quantum Theory of Valence, *Rev. Mod. Phys.* **7**, 167 (1935).
- [13] B. O. Roos, P. R. Taylor, P. E. Sigbahn, A complete active space scf method (casscf) using a density matrix formulated super-ci approach, *Chemical Physics* **48**, 157 (1980).
- [14] B. O. Roos, The complete active space scf method in a fock-matrix-based super-ci formulation, *International Journal of Quantum Chemistry* **18**, 175 (1980).
- [15] S. R. White, Density matrix formulation for quantum renormalization groups, *Physical Review Letters* **69**, 2863 (1992).
- [16] S. R. White, Density-matrix algorithms for quantum renormalization groups, *Physical Review B* **48**, 10345 (1993).
- [17] S. R. White, R. L. Martin, Ab initio quantum chemistry using the density matrix renormalization group, *The Journal of Chemical Physics* **110**, 4127 (1999).
- [18] B. Huron, J. P. Malrieu, P. Rancurel, Iterative perturbation calculations of ground and excited state energies from multiconfigurational zeroth order wavefunctions, *The Journal of Chemical Physics* **58**, 5745 (1973).
- [19] M. Reiher, N. Wiebe, K. M. Svore, D. Wecker, M. Troyer, Elucidating reaction mechanisms on quantum computers,

- Proceedings of the National Academy of Sciences of the United States of America* **114**, 7555 (2017).
- [20] F. Arute, *et al.*, Quantum supremacy using a programmable superconducting processor, *Nature* **574**, 505 (2019).
- [21] G. A. Quantum, Hartree-fock on a superconducting qubit quantum computer, *Science* **369**, 1084 (2020).
- [22] W. J. Huggins, *et al.*, Unbiasing fermionic quantum monte carlo with a quantum computer, *Nature* pp. 1–5 (2022).
- [23] D. Bluvstein, *et al.*, Logical quantum processor based on reconfigurable atom arrays, *Nature* **2023** pp. 1–3 (2023).
- [24] A. Aspuru-Guzik, A. D. Dutoi, P. J. Love, M. Head-Gordon, Simulated quantum computation of molecular energies, *Science* **309**, 1704 (2005).
- [25] A. Y. Kitaev, Quantum measurements and the abelian stabilizer problem, *arXiv:quant-ph/9511026* (1995).
- [26] D. S. Abrams, S. Lloyd, Quantum algorithm providing exponential speed increase for finding eigenvalues and eigenvectors, *Physical Review Letters* **83**, 5162 (1999).
- [27] L. Lin, Y. Tong, Near-optimal ground state preparation, *Quantum* **4**, 372 (2020).
- [28] L. Lin, Y. Tong, Heisenberg-limited ground-state energy estimation for early fault-tolerant quantum computers, *PRX Quantum* **3**, 010318 (2022).
- [29] Y. Dong, L. Lin, Y. Tong, Ground-state preparation and energy estimation on early fault-tolerant quantum computers via quantum eigenvalue transformation of unitary matrices, *PRX Quantum* **3**, 040305 (2022).
- [30] G. Wang, D. S. Frana, R. Zhang, S. Zhu, P. D. Johnson, Quantum algorithm for ground state energy estimation using circuit depth with exponentially improved dependence on precision, *Quantum* **7**, 1167 (2023).
- [31] G. Wang, D. S. Frana, G. Rendon, P. D. Johnson, Faster ground state energy estimation on early fault-tolerant quantum computers via rejection sampling, *arxiv:quant-ph/2304.09827* (2023).
- [32] W. Heitler, F. London, Wechselwirkung neutraler atome und homopolare bindung nach der quantenmechanik, *Zeitschrift fr Physik* **44**, 455 (1927).
- [33] J. Gerratt, General Theory of Spin-Coupled Wave Functions for Atoms and Molecules, *Adv. At. Mol. Phys.* **7**, 141 (1971).
- [34] I. William A. Goddard, T. H. D. Jr., W. J. Hunt, P. J. Hay, Generalized valence bond description of bonding in low-lying states of molecules **6**, 368 (1973).
- [35] J. Li, W. Wu, New algorithm for nonorthogonal ab initio valence-bond calculations I. New strategy and basic expressions, *Theor. Chim. Acta* **89**, 105 (1994).
- [36] I. D. Kivlichan, *et al.*, Quantum simulation of electronic structure with linear depth and connectivity, *Physical Review Letters* **120**, 110501 (2018).
- [37] J.-P. Malrieu, C. Angeli, R. Cimiraglia, On the Relative Merits of Non-Orthogonal and Orthogonal Valence Bond Methods Illustrated on the Hydrogen Molecule, *J. Chem. Educ.* **85**, 150 (2008).
- [38] G. L. Manni, W. Dobrautz, A. Alavi, Compression of spin-adapted multiconfigurational wave functions in exchange-coupled polynuclear spin systems, *Journal of Chemical Theory and Computation* **16**, 2202 (2020).
- [39] J. Paldus, Group theoretical approach to the configuration interaction and perturbation theory calculations for atomic and molecular systems, *J. Chem. Phys.* **61**, 5321 (1974).
- [40] I. Shavitt, Graph theoretical concepts for the unitary group approach to the many-electron correlation problem, *Int. J. Quantum Chem.* **12**, 131 (1977).
- [41] W. D. Laidig, P. Saxe, R. J. Bartlett, The description of n2 and f2 potential energy surfaces using multireference coupled cluster theory, *The Journal of Chemical Physics* **86**, 887 (1987).
- [42] K. Kowalski, P. Piecuch, Renormalized ccSD(t) and ccSD(tq) approaches: Dissociation of the n2 triple bond, *The Journal of Chemical Physics* **113**, 5644 (2000).
- [43] P. Piecuch, S. A. Kucharski, K. Kowalski, Can ordinary single-reference coupled-cluster methods describe the potential energy curve of n2? the renormalized ccSDt(q) study, *Chemical Physics Letters* **344**, 176 (2001).
- [44] H. Larsen, J. Olsen, P. Jrgensen, O. Christiansen, Full configuration interaction benchmarking of coupled-cluster models for the lowest singlet energy surfaces of n2, *The Journal of Chemical Physics* **113**, 6677 (2000).
- [45] G. K. L. Chan, M. Killay, J. Gauss, State-of-the-art density matrix renormalization group and coupled cluster theory studies of the nitrogen binding curve, *The Journal of Chemical Physics* **121**, 6110 (2004).
- [46] L. Bytautas, T. M. Henderson, C. A. Jimnez-Hoyos, J. K. Ellis, G. E. Scuseria, Seniority and orbital symmetry as tools for establishing a full configuration interaction hierarchy, *Journal of Chemical Physics* **135** (2011).
- [47] J. A. Parkhill, K. Lawler, M. Head-Gordon, The perfect quadruples model for electron correlation in a valence active space, *Journal of Chemical Physics* **130**, 84101 (2009).
- [48] G. Gidofalvi, D. A. Mazziotti, Active-space two-electron reduced-density-matrix method: Complete active-space calculations without diagonalization of the n-electron hamiltonian, *Journal of Chemical Physics* **129**, 134108 (2008).
- [49] D. W. Small, M. Head-Gordon, Tractable spin-pure methods for bond breaking: Local many-electron spin-vector sets and an approximate valence bond model, *Journal of Chemical Physics* **130**, 84103 (2009).
- [50] G. H. Booth, A. J. Thom, A. Alavi, Fermion monte carlo without fixed nodes: A game of life, death, and annihilation in Slater determinant space, *Journal of Chemical Physics* **131**, 054106 (2009).
- [51] A. J. W. Thom, Stochastic coupled cluster theory, *Physical Review Letters* **105**, 263004 (2010).
- [52] T. V. Voorhis, M. Head-Gordon, Two-body coupled cluster expansions, *The Journal of Chemical Physics* **115**, 5033 (2001).
- [53] P. ke Malmqvist, A. Rendell, B. O. Roos, The restricted active space self-consistent-field method, implemented with a split graph unitary group approach, *Journal of Physical Chemistry* **94**, 5477 (1990).
- [54] H. Fukutome, Theory of Resonating Quantum Fluctuations in a Fermion System: Resonating Hartree-Fock Approximation, *Prog. Theor. Phys.* **80**, 417 (1988).
- [55] P. Y. Ayala, H. B. Schlegel, A nonorthogonal CI treatment of symmetry breaking in sigma formylxyl radical, *J. Chem. Phys.* **108**, 7560 (1998).
- [56] E. J. Sundstrom, M. Head-Gordon, Non-orthogonal configuration interaction for the calculation of multielectron excited states, *J. Chem. Phys.* **140**, 114103 (2014).
- [57] A. J. W. Thom, M. Head-Gordon, Hartree-Fock solutions as a quasidiabatic basis for nonorthogonal configuration interaction, *J. Chem. Phys.* **131**, 124113 (2009).

- [58] H. G. A. Burton, A. J. W. Thom, General Approach for Multireference Ground and Excited States using Nonorthogonal Configuration Interaction, *J. Chem. Theory Comput.* **15**, 4851 (2019).
- [59] W. D. Laidig, P. Saxe, H. F. Schaefer, III, Multiconfiguration selfconsistentfield study of the importance of triply and quadruply excited electronic configurations in the water molecule, *J. Chem. Phys.* **73**, 1765 (1980).
- [60] P. Saxe, H. F. Schaefer III, N. C. Handy, Exact solution (within a double-zeta basis set) of the schrodinger electronic equation for water, *Chem. Phys. Lett.* **79**, 202 (1981).
- [61] M. Motta, *et al.*, Towards the solution of the many-electron problem in real materials: Equation of state of the hydrogen chain with state-of-the-art many-body methods, *Physical Review X* **7**, 031059 (2017).
- [62] P. A. M. Dirac, Quantum mechanics of many-electron systems, *Proceedings of the Royal Society of London. Series A, Containing Papers of a Mathematical and Physical Character* **123**, 714 (1929).
- [63] P. W. Anderson (Academic Press, 1963), vol. 14 of *Solid State Physics*, pp. 99–214.
- [64] C. L. Cleveland, R. Medina A., Obtaining a Heisenberg Hamiltonian from the Hubbard model, *American Journal of Physics* **44**, 44 (1976).
- [65] M. Motta, *et al.*, Determining eigenstates and thermal states on a quantum computer using quantum imaginary time evolution, *Nature Physics* **16**, 205 (2019).
- [66] M. A. Nielsen, I. L. Chuang, *Quantum Computation and Quantum Information* (Cambridge University Press, 2010).
- [67] S. Lee, *et al.*, Evaluating the evidence for exponential quantum advantage in ground-state quantum chemistry, *Nature Communications* 2023 14:1 **14**, 1 (2023).
- [68] G. H. Low, I. L. Chuang, Hamiltonian simulation by qubitization, *Quantum* **3**, 163 (2019).
- [69] D. W. Berry, C. Gidney, M. Motta, J. R. McClean, R. Babbush, Qubitization of arbitrary basis quantum chemistry leveraging sparsity and low rank factorization, *Quantum* **3**, 208 (2019).
- [70] V. von Burg, *et al.*, Quantum computing enhanced computational catalysis, *Physical Review Research* **3**, 033055 (2021).
- [71] J. Lee, *et al.*, Even more efficient quantum computations of chemistry through tensor hypercontraction, *PRX Quantum* **2**, 030305 (2021).
- [72] S. McArdle, S. Endo, A. Aspuru-Guzik, S. C. Benjamin, X. Yuan, Quantum computational chemistry, *Reviews of Modern Physics* **92**, 15003 (2020).
- [73] J. J. Goings, *et al.*, Reliably assessing the electronic structure of cytochrome p450 on todays classical computers and tomorrows quantum computers, *Proceedings of the National Academy of Sciences of the United States of America* **119**, e2203533119 (2022).
- [74] K. Sugisaki, *et al.*, Quantum chemistry on quantum computers: A method for preparation of multiconfigurational wave functions on quantum computers without performing post-hartreefock calculations, *ACS Central Science* **5**, 167 (2019).
- [75] D. Marti-Dafcik, H. G. Burton, D. P. Tew, Encoding strong correlation in quantum computational chemistry through spin-coupled initial states (2024).
- [76] W. K. Trygve Helgaker, D. P. Tew, Quantitative quantum chemistry, *Molecular Physics* **106**, 2107 (2008).
- [77] F. A. Evangelista, Perspective: Multireference coupled cluster theories of dynamical electron correlation, *Journal of Chemical Physics* **149**, 30901 (2018).
- [78] N. H. Stair, R. Huang, F. A. Evangelista, A multireference quantum krylov algorithm for strongly correlated electrons, *Journal of Chemical Theory and Computation* **16**, 2236 (2020).
- [79] K. Klymko, *et al.*, Real-time evolution for ultracompact hamiltonian eigenstates on quantum hardware, *PRX Quantum* **3**, 020323 (2022).
- [80] K. Andersson, P. ke Malmqvist, B. O. Roos, A. J. Sadlej, K. Wolinski, Second-order perturbation theory with a casscf reference function, *Journal of Physical Chemistry* **94**, 5483 (1990).
- [81] K. Andersson, *et al.*, Secondorder perturbation theory with a complete active space selfconsistent field reference function, *The Journal of Chemical Physics* **96**, 1218 (1992).
- [82] R. J. Bartlett, M. Musia, Coupled-cluster theory in quantum chemistry, *Reviews of Modern Physics* **79**, 291 (2007).
- [83] P. G. Szalay, T. Mller, G. Gidofalvi, H. Lischka, R. Shepard, Multiconfiguration self-consistent field and multireference configuration interaction methods and applications, *Chemical Reviews* **112**, 108 (2012).
- [84] I. Mayer, *Simple Theorems, Proofs, and Derivations in Quantum Chemistry* (Springer, 2003).
- [85] H. G. A. Burton, Generalized nonorthogonal matrix elements: Unifying Wick’s theorem and the Slater–Condon rules, *J. Chem. Phys.* **154**, 144109 (2021).
- [86] H. G. A. Burton, Generalized nonorthogonal matrix elements. II: Extension to arbitrary excitations, *J. Chem. Phys.* **157**, 204109 (2022).
- [87] Q. Sun, *et al.*, Pyscf: the pythonbased simulations of chemistry framework, *WIREs Computational Molecular Science* **8** (2018).
- [88] Q. Sun, *et al.*, Recent developments in the pyscf program package, *The Journal of Chemical Physics* **153**, 024109 (2020).
- [89] W. Humphrey, A. Dalke, K. Schulten, VMD – Visual Molecular Dynamics, *J. Mol. Graph.* **14**, 33 (1996).